CARBON-INFILTRATED CARBON NANOTUBE COATING APPLICATIONS: SCALPEL BLADES AND EXTERNAL FIXATORS

Stephanie R. Morco, Jaclyn M. Larsen, Brian D. Jensen, Anton E. Bowden
Department of Mechanical Engineering, Brigham Young University
Provo, UT

ABSTRACT

A carbon-infiltrated carbon nanotube (CICNT) coating grown on stainless steel has a broad range of possible applications due to its non-pharmaceutical biofilm resistance [1]. This property may provide a solution to surgical site infection (SSI), so scalpel blades and external fixator pins were coated with CICNT and subjected to mechanical testing and MRSA biofilm testing. This scalpel blade coating is one of the first reports of CNT fabrication using 400-series SS as a substrate and a catalyst [2]. The CICNT coating did not prove to have superior anti-bacterial performance to a bare scalpel blade, but this work provides greater insight on CICNT properties. Hardness that was lost during the CICNT manufacturing process was recoverable, and the coating did not delaminate under the force of a diamond scribe. Although the CICNT on these scalpel blades did not exhibit MRSA biofilm resistance, new theories were offered on what factors are critical for the CICNT nanostructure to resist biofilm. The external fixator pin application proved to have significantly more promise than the scalpel blades. The bare stainless steel pin was completely covered in MRSA biofilm, while both the vertically-aligned and randomly-oriented CICNT-coated pins each allowed only a few cells to attach. Although there is more testing to be done, a CICNT coating may be an exceptional way to prevent infection while reducing antibiotic use.

Corresponding author: Anton E. Bowden

1. INTRODUCTION

1.1 The Need for an Antibacterial Coating

Surgical site infection (SSI) continues to affect hundreds of thousands of people in the US each year [1]. With a 2-5% incidence rate and $3.5-$10 billion annual US cost, these infections are now the most common and costly type of hospital-acquired infection [1, 2]. For orthopaedic joint replacements, approximately half of SSIs are periprosthetic joint infections (PJIs) [3], which may be considered the most devastating complication of these surgeries [4]. The bacteria species that cause most SSI and PJI are part of the normal skin flora [5, 6], so although the evidence is limited, the scalpel may potentially cause some of these infections [7]. Therefore, coating a scalpel with an antibacterial coating may prove beneficial.

Along with addressing the scalpel as an infection source, external fixator pins have a remarkably high infection rate. The pin tract infection rate is 21% to 42% of cases [8]. Yet despite this risk inherent with the device's transdermal pathway, they are still used because they play an important role in cases that need reduced soft tissue damage, avoidance of any infected areas, and

Copyright 2020. Used by the Society of the Advancement of Material and Process Engineering with permission.

adjustability [9]. Therefore, coating an external fixator pin with an antibacterial coating may also prove beneficial.

1.2 Challenges with Current Solutions

There are a variety of efforts aimed at addressing the challenge of SSI for external fixator pin infection. Coating pins with silver, iodine, or gentamicin-coated sleeves has shown evidence of reducing infection [10]. However, all of these options are based on their chemistry, so there is a concern of cytotoxic effects [11]. Additionally, antibiotic-based coatings are limited by drug-resistant bacteria strains, such as methicillin-resistant S. aureus (MRSA), and biofilm formation that makes systemic antibiotics ineffective [11].

1.3 Benefits of a CICNT Coating

A carbon-infiltrated carbon nanotube (CICNT) coating may offer an improved solution. Recent in vitro testing on CICNT coatings provides evidence that this coating resists MRSA cell attachment and biofilm formation due to its nanostructure rather than its chemistry [12]. Although additional testing is required, the results are promising, especially because it can be easily coated directly onto stainless steel (used in both scalpel blades and external fixation pins) and on different geometries. Other advantages of a CICNT coating include that it is low cost [13], heat stable, and would have a theoretically infinite shelf life. Because of this, potential applications are being investigated. The objective of this research is to test the feasibility and effectiveness of coating scalpel blades and/or external fixator pins with CICNT to resist bacterial infection.

2. EXPERIMENTATION

2.1 Scalpel Blade Fabrication and Testing

CICNT was coated directly onto size 10 scalpel blades with a process optimized for this 400-series stainless steel (SS). The process sequence was a heat treatment, CNT growth, then carbon infiltration, all in a CVD tube furnace. The heat treatment was at 800°C in argon (Ar, flowing at 250 sccm) for 30 minutes, the CNT growth was at 700°C in hydrogen (H2, flowing at 230 sccm) and ethylene (C2H4, flowing at 250 sccm) for 15 minutes, and the carbon infiltration was at 850°C in Ar and C2H4 for 25 minutes. Controls were uncoated size 10 scalpel blades.

The CICNT coatings on scalpel blades then underwent various mechanical tests: cutting performance, hardness changes, and scratch durability. Cutting performance was tested by an experienced dissection technician cutting raw chicken with the skin intact using two coated and two uncoated blades. Four types of cuts were performed: plunge cut, 4-6 inch longitudinal cut, skin and tissue separation cut, and a cut that strikes the bone. This allowed for a subjective feedback on cutting feel and sharpness. Hardness change was tested on a Rockwell C scale in five locations (two on the body and three along the edge of the blade) on two of each type of treatment: (1) uncoated scalpels, (2) heat treated scalpels that underwent the time-temperatures protocol for growing CICNT, but without the carbon source, (3) CICNT-coated scalpels, (4) heat treated scalpels quenched in oil directly following the “infiltration” step, and (5) CICNT-coated scalpels quenched in oil directly following infiltration. The CICNT coating’s scratch durability was tested with a diamond scribe scratching a coated scalpel blade nine times: three different pressures (light, medium, strong) in three locations. These were then SEM imaged for visual results.

Finally, the scalpel blade coating was tested for MRSA biofilm resistance. Three coated and uncoated scalpel blades were placed in a CDC biofilm reactor with MRSA-inoculated tryptic soy broth (TSB). The reactor was placed on a hot plate set to 34°C and 130 rpm for 24 hours. To prepare for SEM imaging, samples were rinsed in phosphate-buffered saline (PBS), fixed with glutaraldehyde, dehydrated with ethanol, and coated with gold [14]. SEM images were taken at 5000x magnification in five locations: three along the sharpened edge and two on the body of the blade. This magnification was used to view the morphology and spread of MRSA cells.

2.2 External Fixator Pin Fabrication and Testing

External fixator pins were coated with CI-CNT using two CNT catalyst methods: layered and direct. The pins were 316L SS rods (McMaster 89325K91) with a 0.25-inch diameter and approximately 1-inch length. An uncoated SS rod was used as a control.

The layered method produced a CNT forest by a using a traditional, externally-applied catalyst [15]. First, a diffusion barrier, an 80-nm thick layer of alumina, was deposited onto the pins by rotating the pins during an electron-beam deposition [15]. The pins were also rotated during the thermal evaporation of the CNT catalyst, a 4 nm thick layer of iron. A CNT forest was grown then infiltrated in a CVD tube furnace. The growth occurred at 750°C with hydrogen (flowing at 230 sccm) and ethylene (flowing at 250 sccm) for 1 minute, and the infiltration occurred at 900°C under the same gases and flow rates for 22 minutes.

The direct method produced a CNT forest by modifying the SS substrate to be a catalyst – similar to the scalpel blade coating fabrication. This was performed in the CVD furnace in continuity: heat treatment, CNT growth, then CNT infiltration. The heat treatment occurred at 800°C with air (flowing at approximately 200 sccm) for 5 minutes, the CNT growth occurred at 700°C with hydrogen (flowing at 230 sccm) and ethylene (flowing at 250 sccm) for 15 minutes, and the CNT infiltration occurred at 850°C with argon (flowing at 250 sccm) and ethylene (flowing at 250 sccm) for 25 minutes.

Three external fixator pins were tested for MRSA biofilm resistance – one of each type of pin. A pin that was coated by the layered method, one that was coated by the direct method, and one uncoated pin as a control were fixed to coupons using paraffin wax then placed in a CDC biofilm reactor under the same conditions as the scalpel blades for the first 24 hours. For the subsequent 24 hours, the nutrients in the broth were replenished by flowing fresh TSB diluted to 10% strength (~6.9 mL/min). After 48 hours, the pins were prepared for SEM imaging using the same process as the scalpels above. SEM images were consistently taken at the apex of the pins at 1,000x and 10,000x to view the morphology and spread of MRSA cells.

3. RESULTS AND DISCUSSION

3.1 Scalpel Blades

3.1.1 CICNT Coating Morphology

The CICNT coating on the scalpel blades was randomly-oriented and mostly uniform (Figure 1). There were no distinct patches of overgrown CICNT that are sometimes called bush-like growths [17]. Another observation was that the body of the blades had longer CICNT and more CICNT height variation than the edge of the blades. A randomly-oriented forest was expected because

most methods for growing CNT using SS as the substrate and catalyst do not produce vertically-aligned forests [18]. Because the surface structure is still similar to vertically-aligned CICNT on the nanoscale, a randomly-oriented forest has previously shown evidence of biofilm resistance properties [1].

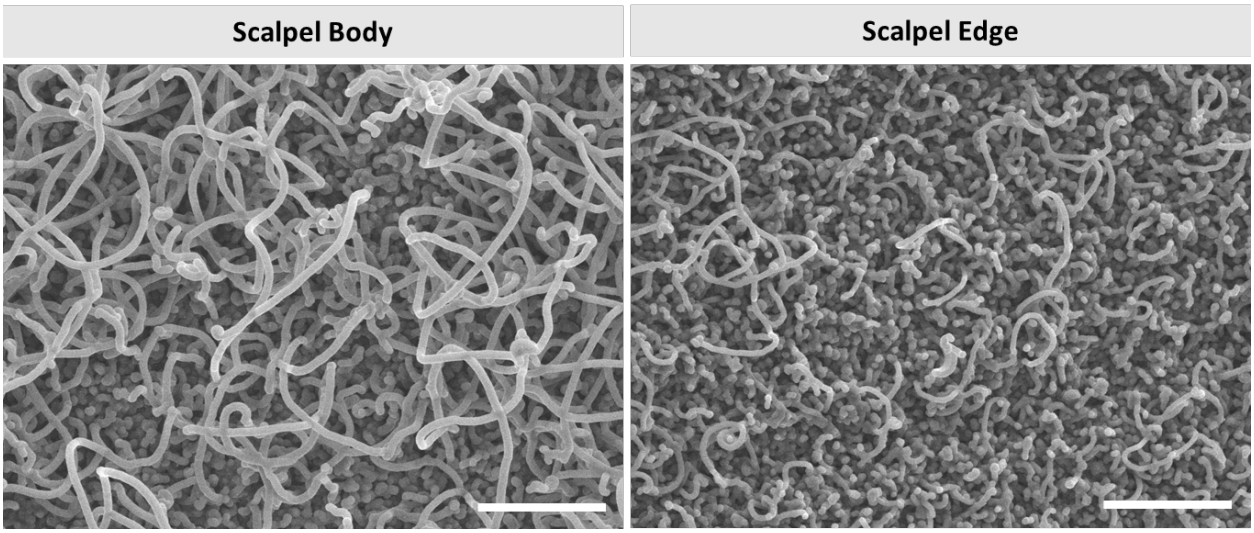


Figure 1: Top view of the body (left) and blade edge (right) of a CICNT-coated scalpel blade. Scale bars are 5 μm (10,000x magnification).

3.1.2 Cutting Performance

An experienced dissection technician performed the various cuts through raw chicken using the CICNT-coated scalpel blades to test their function. The coated and uncoated blades successfully dissected the chicken using a plunge cut, a 4-6 inch longitudinal cut, a skin and tissue separation cut, and a cut that strikes the bone. There were no black spots indicating detachment of CICNT in the chicken; however, the technician feedback indicated that the coated blades were less sharp than the uncoated blades. Since a blade's sharpness over prolonged use is directly correlated to its hardness, this prompted a look into a hardness recovery process for the CICNT-coated blades. This is detailed in the next section.

3.1.3 Scalpel Hardness

The CICNT fabrication process may affect the scalpel's hardness, and because a material's hardness determines how sharp a blade stays, this property was investigated. The hardness of a blade with no treatment ("Uncoated") was compared to four other treatments. Two treatments were treated and cooled in the furnace ("Heat Treat" and "CICNT"), and two treatments were quenched in oil after the 800°C infiltration in order to harden the blades ("Heat Treat & Quench" and "CICNT & Quench"). The oil quenched blades showed increased hardness (Figure 2). The blades that went through the CICNT process without carbon gas ("Heat Treat" and "Heat Treat & Quench") each show decreased hardness compared to their CICNT counterparts (Figure 2).

The results indicated that the temperatures required to coat scalpels with CICNT significantly reduce the hardness of the blade, but this hardness can be almost completely recovered. The heat treatment without CICNT reduced the hardness from an average of 53 HRC to an average of 31

HRC. The carburizing from the ethylene during the growth and infiltration of CICNT caused the hardness to increase to an average of 41 HRC. Approximately the same amount of hardness could be recovered by an oil quench directly following the "infiltration" step during the heat treatment (average of 43 HRC). The hardness was nearly recovered by combining the carburizing from the CICNT growth and infiltration with the oil quench directly following the infiltration step (average of 48 HRC). This shows that a CICNT-coated scalpel blade could be nearly as capable at maintaining a sharp edge.

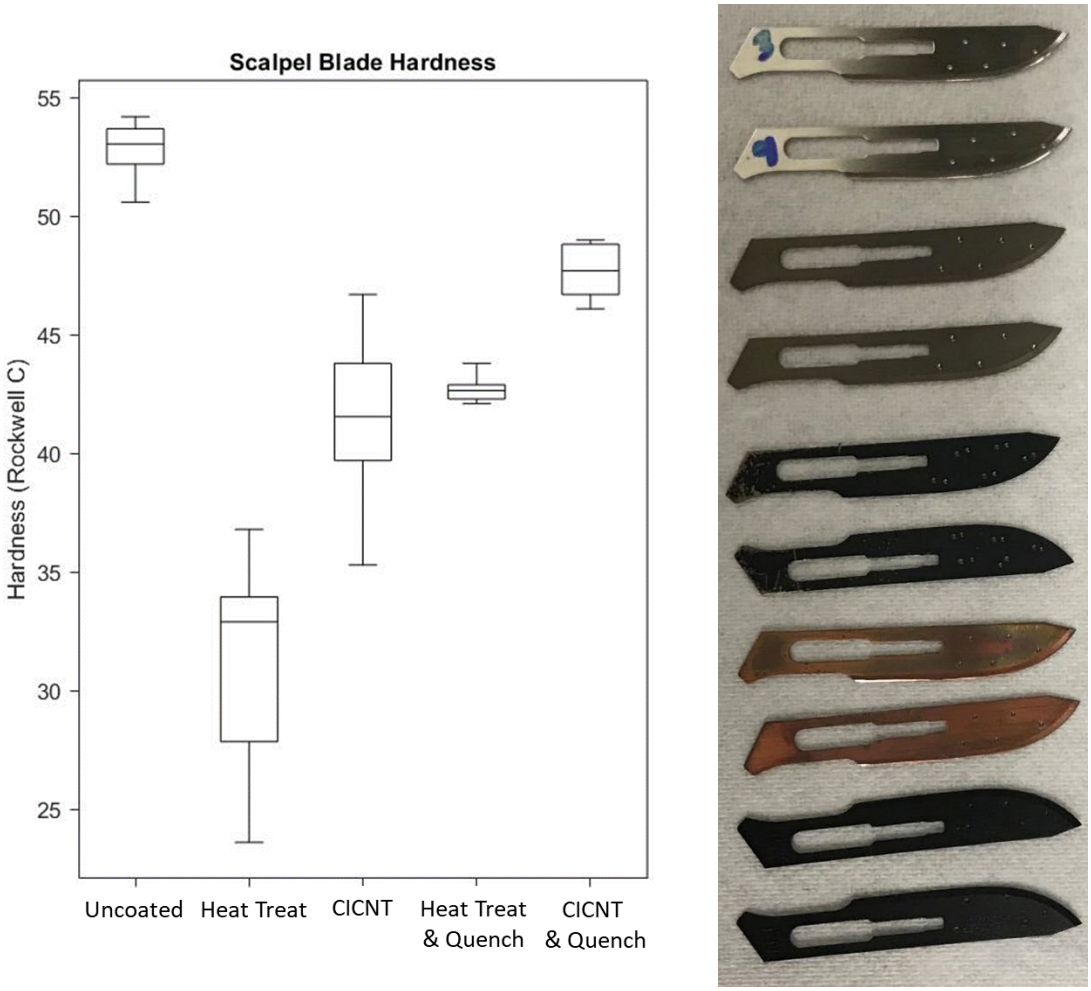


Figure 2: Scalpel hardness measurements for various treatments (left). Photo of the scalpel blades measured (right). Indentations show the measurement locations. Treatment pairs from top to bottom: uncoated, heat treated, CICNT-coated, heat treated and quenched, CICNT-coated and quenched.

3.1.4 Scratch Durability

CICNT-coated scalpel blades were able to withstand the hardness of a diamond scribe scratch with only a local disturbance rather than delamination. SEM images of the scratches are shown in Figure 3. As the force increased, both surfaces naturally exhibited a deeper and wider disturbance. Compared to bare scalpel, the disturbance was wider on the CICNT-coated blade than the uncoated

blade. As measured in the previous section, the hardness of the CICNT-coated blades is reduced without an oil quench, so the wider disturbance may be due to the 12 HRC reduction in hardness.

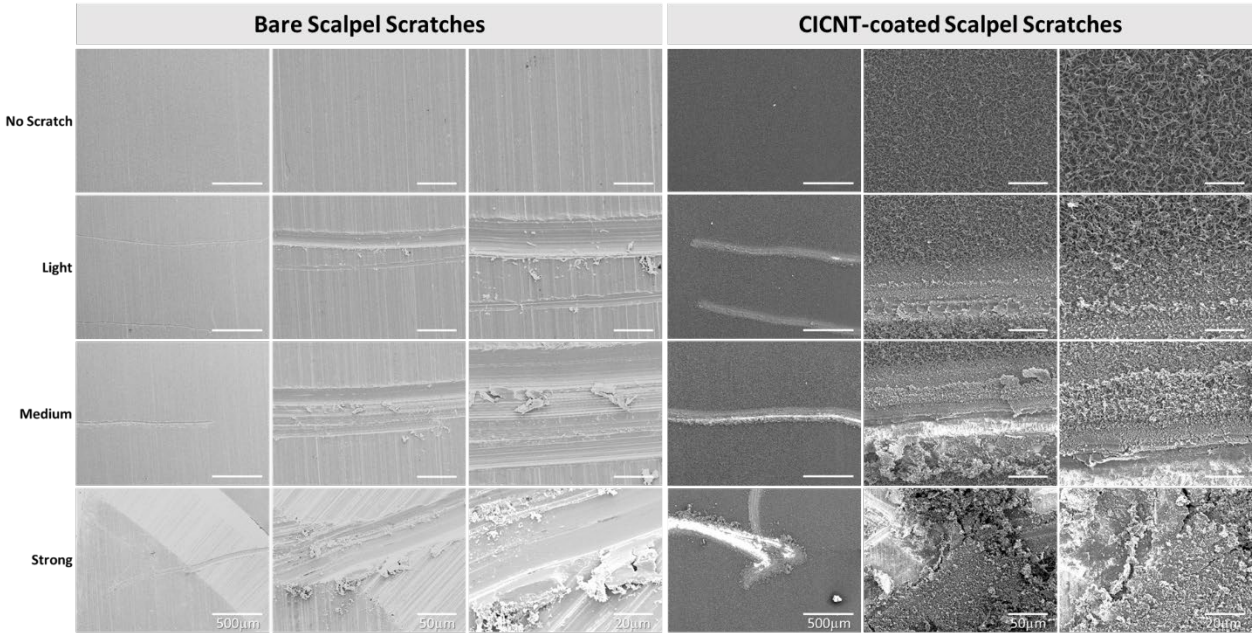


Figure 3: SEM images of scratched scalpels. Bare scalpel scratches (left set of images) and CICNT-coated scalpel scratches (right set of images) with increasing magnifications left to right (scale bars: 500 µm, 50 µm, and 20 µm for each set) and increasing pressures top to bottom (no scratch, light pressure, medium pressure, and strong pressure) are shown.

3.1.5 MRSA Biofilm Resistance

Following 24 hours in the MRSA biofilm reactor, the CICNT-coated scalpels allowed more biofilm attachment than the uncoated scalpels (Figure 4); however, comparing these results to a CICNT coating that resists biofilm expands our understanding on critical dimensions needed for a nanostructure to resist MRSA biofilm. The main difference between the scalpel coating and other successful CICNT coatings is that the CICNT heights on the scalpels were significantly more variable. This variation allowed the longer nanotubes to spread out throughout the surface, and this may affect the results in a variety of ways.

Because biofilm formation is directly related to the shear stress caused by the fluid dynamics from the rotating paddle [19], the flow dynamics at the surface may be different on this CICNT-coating than on the CICNT-coated fixator pins (Section 4.2) or on the coatings reported in previous experiments [1]. The additional roughness caused by the extra-long CICNT may have altered the shear stress to a more optimal level for biofilm formation. The individual CICNT may have caused additional flow disturbances on the nanoscale as the broth flowed over all the nanotubes.

Because biofilm formation is also directly related to the stiffness of its substrate [20], the unusual result could be caused by the lower stiffness in the longer nanotubes. There is an optimal stiffness for S. aureus biofilm formation [20], and MRSA most likely has the same response. Modeling the extra-long nanotubes as beams, their stiffness would be significantly reduced because the length

of the beam, or nanotube, variable is to the fourth power. Therefore, although CICNT has a high modulus of elasticity [21], the stiffness of the scalpel blade coating may have changed enough to become optimal for MRSA biofilm formation.

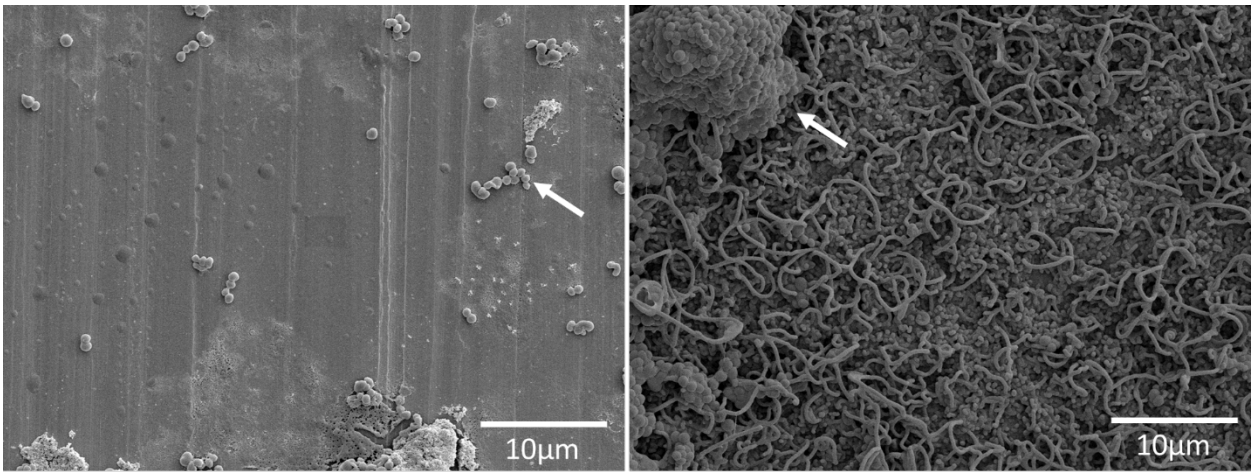


Figure 4: SEM images taken on the body of the uncoated (left) and CICNT-coated (right) scalpels after 24 hours in a MRSA biofilm reactor. The largest groups of MRSA cells on each image are indicated by arrows. The CICNT-coated blade had more biofilm formation.

3.2 External Fixator Pins

3.2.1 CICNT Coating Morphology

The CICNT fabrication method using a layered catalyst produced a vertically-aligned forest, and the method using a direct catalyst produced a randomly-oriented forest. SEM images of these are shown in the left columns of Figure 5. The CICNT forest from the layered method has relatively smooth and uniform surface, whereas the CICNT forest from the direct method shows bush-like growths.

3.2.2 MRSA Biofilm Resistance

Following 48 hours in a MRSA biofilm reactor, SEM images of the fixator pins showed significantly less biofilm formation for both types of CICNT coatings compared to the bare SS pin (Figure 5). MRSA cells were identified by their spherical shape, smooth edges, and roughly 0.8µm diameter, and then marked in Figure 6. The bare SS pin was entirely covered with MRSA cells, while there are only a handful of cells on the pins with a CICNT coating. The cell aggregation on the bare SS pin indicated mature biofilm formation on the surface, and the lack of cells attached to both types of CICNT coating indicated biofilm resistance. This biofilm resistance has an advantage over other anti-bacterial coatings, such as pharmaceuticals or silver, because its mechanism does not kill the bacteria.

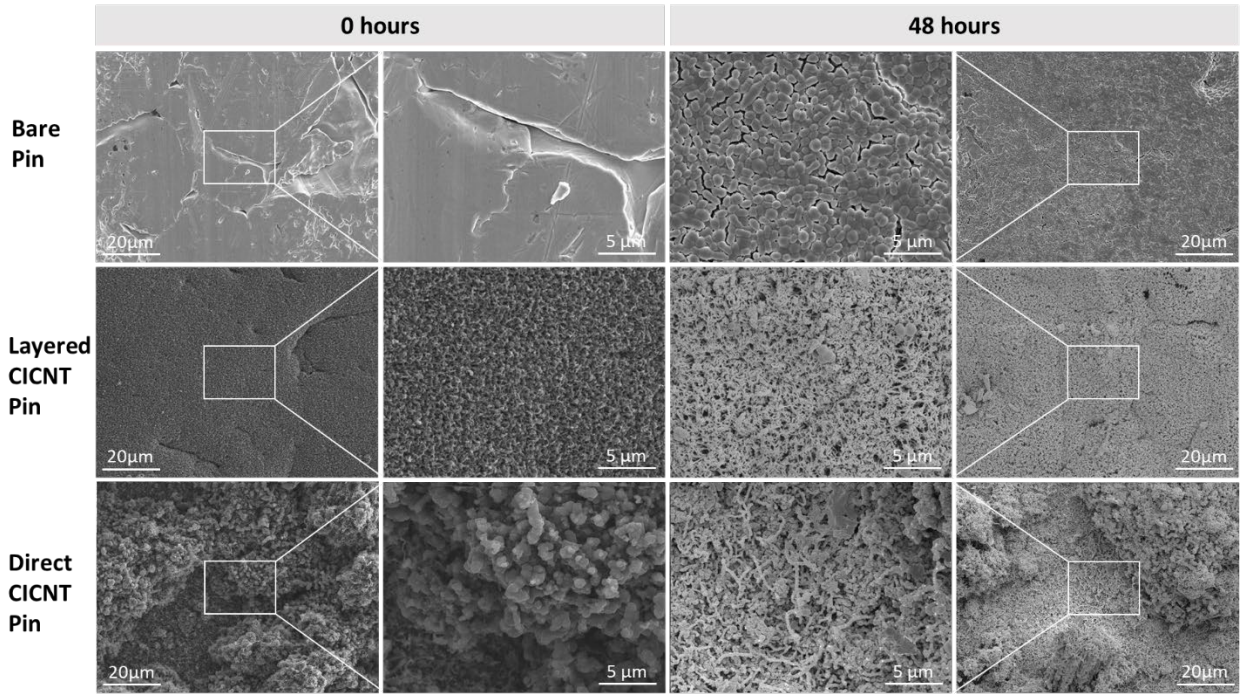


Figure 5: SEM images of each material before (left) and after (right) the experiment. After 48 hours, MRSA cells were identified by their spherical shape, smooth edges, and roughly 0.8µm diameter. Magnifications are 1,000x and 10,000x.

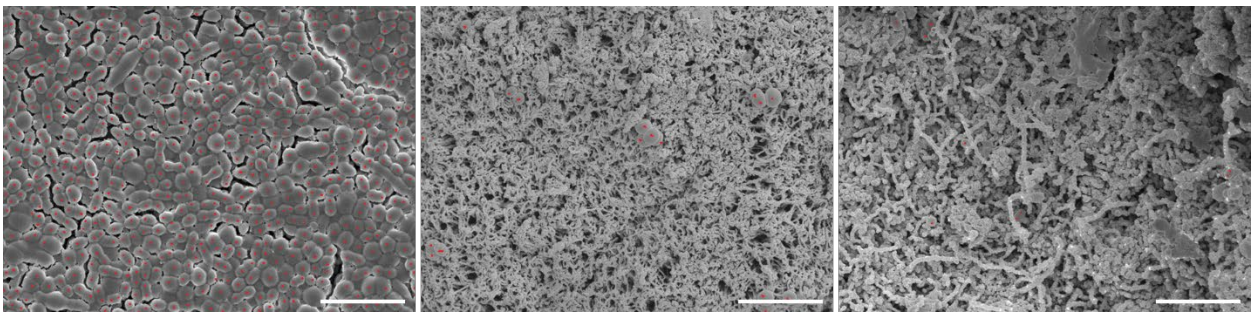


Figure 6: MRSA cells marked in red for each material: bare SS, layered CICNT pin, and direct CICNT pin. Image locations are the same as those in Figure 5. Scale bars are 5 µm.

3.3 Limitations and Future Work

As with any study of a new coating, there are limitations that provide more areas to research. More extensive testing must be done to further understand and verify the MRSA biofilm resistance seen from CICNT coatings. In general, these tests would include additional variables such as physical variations of CICNT, higher sample sizes, additional bacterial strains, and multiple experiment lengths. Specifically, since this study showed exceptional MRSA biofilm resistance on external fixator pins coated with CICNT, more testing must be done to ensure that the CICNT coatings promote skin-implant integration because infection is regularly the result of this lack of integration [22].

The disturbance of the CICNT coating caused by the diamond scribe during the scratch durability testing likely removed some CICNT from the substrate. This may be a problem in vivo if the infiltration is removed from the CICNT to expose the CNT to the body. Although CICNT have shown biocompatibility, it is questionable if bare CNT is biocompatible because the evidence is inconclusive and there are multiple factors that affect its toxicity [23, 24]. Additional testing would need to be done.

4. CONCLUSIONS

Because CICNT-coating that has been shown to resist biofilm formation based on its nanostructure rather than its chemistry [1], a solution for SSI was proposed by coating scalpel blades and external fixator pins with CICNT and subjecting them to mechanical and MRSA biofilm tests. On the scalpel blades, the CICNT coating did not exhibit superior performance to a bare scalpel blade, but this work provides greater insight on CICNT properties. The hardness that was lost during the CICNT manufacturing process was recoverable, and the coating did not delaminate under the force of a diamond scribe. Although the CICNT-coating on scalpel blades did not show MRSA biofilm resistance, the variables critical for the CICNT nanostructure to resist biofilm are better understood. The external fixator pin application proved to have significantly more promise than the scalpel blades. The bare SS pin was completely covered in MRSA biofilm, while both the vertically-aligned and randomly-oriented CICNT-coated pins each allowed only a few cells to attach. Although there is more testing to be done, we are optimistic that a CICNT coating will prove to be an exceptional way to prevent infection while reducing antibiotic use.

5. REFERENCES

1. Morco, S., et al., Structural Antibacterial Properties of Carbon-Infiltrated Carbon Nanotube Coatings, in BMES. 2016.
2. Hu, J.J., et al., Tribological behavior and graphitization of carbon nanotubes grown on 440C stainless steel. Tribology Letters, 2005. DOI: 10.1007/s11249-005-5091-6.
3. Ban, K.A., et al., American College of Surgeons and Surgical Infection Society: Surgical Site Infection Guidelines, 2016 Update. J Am Coll Surg, 2017. DOI: 10.1016/j.jamcollsurg.2016.10.029.
4. Anderson, D.J., et al., Strategies to prevent surgical site infections in acute care hospitals: 2014 update. Infect Control Hosp Epidemiol, 2014. DOI: 10.1086/676022.
5. Dryden, M., Prosthetic joint infection: managing infection in a bionic era. J Antimicrob Chemother, 2014. DOI: 10.1093/jac/dku246.
6. Bjerke-Kroll, B.T., et al., Periprosthetic joint infections treated with two-stage revision over 14 years: an evolving microbiology profile. J Arthroplasty, 2014. DOI: 10.1016/j.arth.2013.09.053.
7. Tande, A.J. and R. Patel, Prosthetic joint infection. Clin Microbiol Rev, 2014. DOI: 10.1128/CMR.00111-13.
8. Calina, D., et al., Antimicrobial resistance development following surgical site infections. Mol Med Rep, 2017. DOI: 10.3892/mmr.2016.6034.

9. Alaee, F., et al., General Assembly, Prevention, Operating Room - Surgical Technique: Proceedings of International Consensus on Orthopedic Infections. J Arthroplasty, 2019. DOI: 10.1016/j.arth.2018.09.064.
10. Guerado, E., J.R. Cano, and F. Fernandez-Sanchez, Pin tract infection prophylaxis and treatment. Injury, 2019. DOI: 10.1016/j.injury.2019.03.044.
11. Bliven, E.K., et al., External fixation of the lower extremities: Biomechanical perspective and recent innovations. Injury, 2019. DOI: 10.1016/j.injury.2019.03.041.
12. Shirai, T., et al., Prevention of pin tract infection with iodine-supported titanium pins. J Orthop Sci, 2014. DOI: 10.1007/s00776-014-0561-z.
13. Jennison, T., M. McNally, and H. Pandit, Prevention of infection in external fixator pin sites. Acta Biomater, 2014. DOI: 10.1016/j.actbio.2013.09.019.
14. Baddour, C.E., et al., A simple thermal CVD method for carbon nanotube synthesis on stainless steel 304 without the addition of an external catalyst. Carbon, 2009. DOI: https://doi.org/10.1016/j.carbon.2008.10.038.
15. Williams, D.L. and R.D. Bloebaum, Observing the Biofilm Matrix of Staphylococcus epidermidis ATCC 35984 Grown Using the CDC Biofilm Reactor. Microscopy and Microanalysis, 2010. DOI: 10.1017/S143192760999136x.
16. Robison, W., B. Jensen, and A. Bowden, Patterned Carbon Nanotube Growth on Convex Cylindrical Stainless Steel Substrates for the Production of Coronary Stents. 2016. DOI: 10.1115/DETC2016-60243.
17. Prawitt, D.G., D. Porter, and B.D. Jensen, Patterned Carbon Nanotube Growth on Stainless Steel in International Design Engineering Technical Conferences and Computers and Information in Engineering Conference. ASME: Quebec City, Quebec, Canada. 2018 DOI: https://doi.org/10.1115/DETC2018-86130.
18. Zhuo, C., et al., Oxidative heat treatment of 316L stainless steel for effective catalytic growth of carbon nanotubes. Applied Surface Science, 2014. DOI: 10.1016/j.apsusc.2014.05.189.
19. Williams, D.L., et al., Growth substrate may influence biofilm susceptibility to antibiotics. PloS one, 2019. DOI: 10.1371/journal.pone.0206774.
20. Yu, C., et al., Nanoprobe-based force spectroscopy as a versatile platform for probing the mechanical adhesion of bacteria. Nanoscale, 2019. DOI: 10.1039/c8nr10338k.
21. Hanna, B.H., et al., Mechanical Property Measurement of Carbon Infiltrated Carbon Nanotube Structures for Compliant Micromechanisms. Journal of Microelectromechanical Systems, 2014. DOI: 10.1109/jmems.2014.2312847.
22. Peramo, A. and C.L. Marcelo, Bioengineering the skin-implant interface: the use of regenerative therapies in implanted devices. Ann Biomed Eng, 2010. DOI: 10.1007/s10439-010-9937-1.
23. Mohanta, D., et al., Carbon nanotubes: Evaluation of toxicity at biointerfaces. Journal of Pharmaceutical Analysis, 2019. DOI: https://doi.org/10.1016/j.jpha.2019.04.003.

24. Ignat, S.R., et al., Versatile Biomaterial Platform Enriched with Graphene Oxide and Carbon Nanotubes for Multiple Tissue Engineering Applications. Int J Mol Sci, 2019. DOI: 10.3390/ijms20163868.